Advanced Measurement, Characterization and Simulation of Thermoplastic Composite Induction Welding

Yun Wan, Steven Liu
Institute of Control Systems, University of Kaiserslautern, Kaiserslautern, Germany

Martina Hümbert*, Miro Duhovic and Peter Mitschang
Institute for Composite Materials, Kaiserslautern, Germany

* Corresponding author. E-mail: martina.huembert@ivw.uni-kl.de
Received: 18 August 2014; Accepted: 9 September 2014; Published online: 29 September 2014

Abstract
Induction welding is a highly versatile thermoplastic composite (TPC) and hybrid material (metal to composite) fusion bonding process which uses electromagnetic phenomena to generate contact-free heating of the joining partners. Two highly influential sets of parameters in the process are the 'actual' applied coil current amplitude and frequency along with the temperature and frequency dependent electrical conductivity behavior of the joining materials. Both sets of data are not easily measurable and may change dynamically during the process. One of these issues can be addressed from an electrical engineering point of view, which focusses on the induction heating equipment itself and accurate measurement of the electrical behavior of the induction heating circuit. Magnetoresistive sensors especially designed for high-frequency current measurement can be used to measure the coil current and its corresponding waveform for any welding setup. The data recorded by the sensor board, together with Fourier Transform analysis techniques, provides accurate values for the coil current and frequency, which can then be used for process and equipment design simulations assisting in the development of suitable control systems and overall process optimization.

Keywords: *Induction welding, Thermoplastic composites, Current measurement*

1 Introduction

Thermoplastic composite materials are becoming increasingly important in multi-material designs where the overall goal is to reduce component weight. In order to manufacture assemblies which consist of different materials, special joining techniques are necessary. One of these techniques is induction welding. The principle of induction heating can be described as follows. An alternating voltage is placed across a conductive coil and produces an alternating current (AC). The AC generates an alternating time-variable magnetic field with the same frequency. Due to the alternating magnetic field, eddy currents are induced in an electrically conductive workpiece placed close to the coil. In the case of thermoplastic composites, the closed-loop circuits required to form a conductive resistance network exist via the reinforcement weaves or cross plies and eddy currents flow through these fiber circuits producing heat [1,2].

Induction welding is a highly dynamic process that requires a high frequency and amplitude of the current passing through the coil. The induction heating device at the Institut für Verbundwerkstoffe (IVW) GmbH can offer a wide frequency range from hundreds of kHz to almost 1 MHz and a flexible current

Please cite this article as: Y. Wan, S. Liu, M. Hümbert, M. Duhovic, and P. Mitschang, "Advanced Measurement, Characterization and Simulation of Thermoplastic Composite Induction Welding," *KMUTNB Int J Appl Sci Technol*, Vol.7, No.4, pp. 1-12, (2014), http://dx.doi.org/10.14416/j.ijast.2014.09.001

range up to 100 A. In order to understand the process, three important aspects must be considered. First, the influence of a high coil current frequency is regarded. In [3], Rudolf et al. found that the carbon-fiber reinforced thermoplastic cannot be heated beyond 50°C at 20 kHz but can be heated to 300°C at 1.1 MHz in about 5 seconds. These results show that a high coil current frequency leads to high heating rates, which are favorable for industrial mass production. Second, the amplitude of the coil current, which is equivalent to the generator power for a fixed generator voltage, must be taken into account. The experiments in [3] show that it remarkably influences the induction heating process. As the coil current with its high frequency and amplitude generates a strong electromagnetic field, most of the general-purpose electronic devices do not work properly or their precision is greatly reduced. Third, induction welding of TPCs is far from a stationary process. Instead, it involves a complicated heat distribution in the TPC, a nonlinear temperature rise at the welding zone and a highly dynamic process during welding, which is more complicated than heating an iron cooking pot due to the material characteristics of TPCs. These three aspects determine that induction welding of TPCs is a complex process with high technical requirements.

In order to realize an accurate and high-efficient induction welding system, it is important to know the internal physical variables during the welding process from a control engineer's point of view. As mentioned before, the most influential and fully controllable variable is the current through the coil. In [4], the principle of transformers is applied to understand the electrical aspect of induction welding. The coil can be treated as the primary-side winding of a transformer while the TPC represents the secondary-side winding with its load resistance. An accurate understanding of the load characteristics of different TPCs can then be developed using their equivalent electrical circuit based on the transformer principle. It should be mentioned that the parameters of the electrical circuit model vary apparently during the welding process. That is even the case for a determined coil and TPC due to a possible instability of the heating frequency, a changing distance and relative position between coil and TPC, a temperature and frequency dependent material conductivity and so on. When the coil current and voltage are measured and an equivalent electrical circuit is established, a precise process control for welding TPCs can be developed and implemented. However, as to the authors' knowledge, so far no publication has covered the issue of measuring and investigating the coil current for welding TPCs. Additionally, most of the available induction welding equipment does not aim to support a precise induction welding of TPCs and fails to give sufficient information about the coil current. In some cases, only the power consumption of the inverter is displayed, in other instances, the current which flows through the DC-link of the inverter is displayed. Although the latter case is already an improvement, it does not indicate the amount of the power flowing into the TPC, which causes the temperature rise. Therefore, a measurement and data acquisition system should be custom-made to the IVW induction welding device for measuring coil current and voltage.

There are many difficulties in measuring the highly dynamic, high amplitude (up to 100 A) and high frequency (100 kHz-1 MHz) currents of the induction coil with limited installation space and comparatively high precision. The measurement also needs to be performed in a strong electromagnetic environment induced by the coil current. Most of the available sensors, such as instrument shunts and Hall sensors are not suitable for that application. The authors in [5] developed a 1.5 MHz-3.5 kW resonant inverter for induction heating, where voltage and current measurements were performed by expensive Tektronix probes [6]. The measurement data was collected by a 1 GHz-bandwidth 10 Gs/s-sampling-rate oscilloscope, calibrated for accurate results and used to construct the equivalent impedance parameters of a ferromagnetic pot on the heater. The IVW induction welding system has a higher power rating (10 kW), an enclosed structure for safety and limited space to install additional measurement devices. Therefore, the existing inverter system needs to be specially and appropriately adapted for the implementation of a measurement system. In addition, suitable sensors are required to measure the coil current and voltage without being influenced by the existing strong electromagnetic field.

This paper presents a method to measure the current directly on the coil as a first step towards achieving a deeper understanding of the induction heating behavior of TPCs. First, a suitable sensor board is chosen; second, a solution for installing the sensor

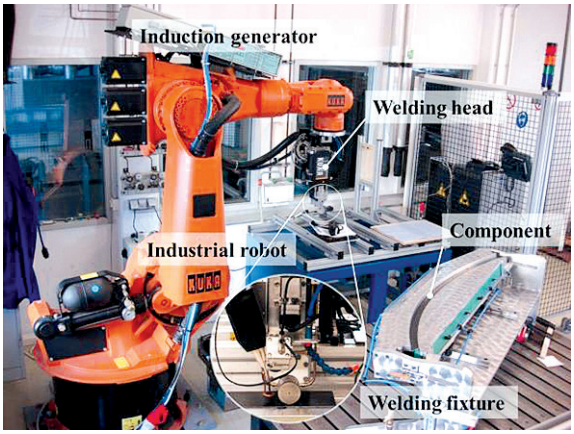

Figure 1: Induction welding as performed by an industrial robot.

board between the inverter and coil is developed; and third, experiments are performed to verify the method and the test setup. In addition, a framework of simulation techniques is proposed which can predict the heating behavior using the measured current as simulation input.

2 State of the Art

2.1 *State of the art of induction welding*

In order to use induction heating for an automated welding process, the radio frequency (RF) power supply and its coil must be combined with a pressure unit. This can be a stamp or a consolidation roller. The latter is used for continuous induction welding. The process is automated by attaching a welding head to an industrial robot, as shown in Figure 1.

The welding head (Figure 2) contains the roller and the coil and is moved along a weld seam by the robot. The coil then heats the laminate stack until the polymer melts and the consolidation roller subsequently reconsolidates and cools the material. In this way, the two laminates can be joined.

There are several different parameters that define this welding process:

(1) The current on the coil, as described in the introduction, is one of the most important parameters during heating which is of course the case also during welding.

(2) The distance between the coil and the workpiece is as important as the current, but it can be measured easily.

(3) The movement of the robot defines the current which is needed to heat the material up to melting temperature. High speeds require a high power input and therefore a high coil current. But a high speed also reduces the amount of heat which can be removed by the consolidation roller.

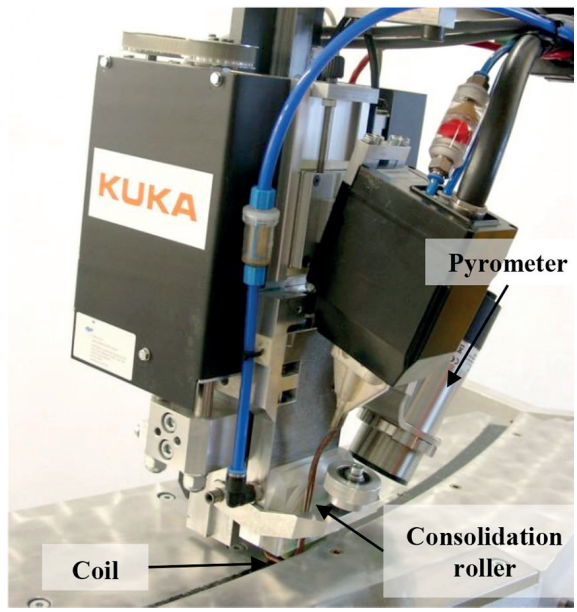

Figure 2: Induction welding head.

In addition to these process parameters, the electromagnetic properties of the material to be welded also play an important role. The material must be either magnetic or electrically conductive or both. In composites, one of these criteria is satisfied in the case of carbon fibers as long as they form closed current circuits, as they do in a reinforcement weave. Therefore, carbon fiber woven reinforcements can be heated and welded without the use of any additional materials. Glass fibers, in contrast, are neither electrically conductive nor magnetic. Thus, an additional material, a so called susceptor, must be added. A commonly used susceptor is a metal mesh which is placed in the welding zone between two glass fiber reinforced laminates. Due to the material dependency of the process, the material properties giving rise to whichever heating mechanism is used must be investigated in order to adapt the process.

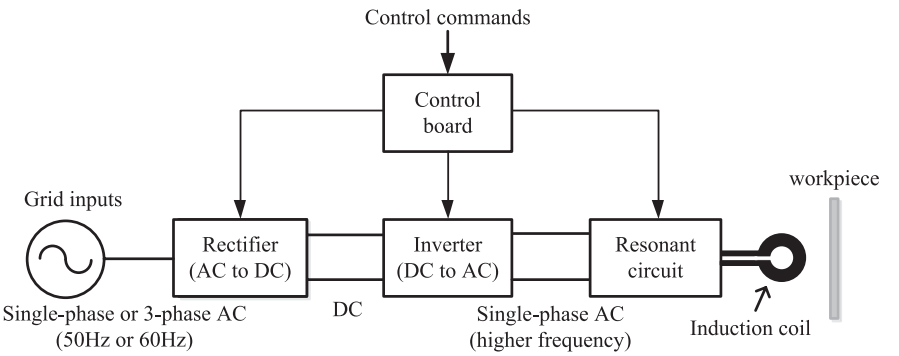

Figure 3: Basic block diagram of an RF power supply.

2.2 *Commercially available induction heating systems*

The central component of an induction welding system is the RF power supply. Generally, a RF power supply can be classified as a resonant power converter. It implements a frequency change from the available fixed AC voltage to a single-phase voltage at a specified high frequency, which is appropriate for the induction heating process [7]. Figure 3 shows a basic block diagram for a generalized modern RF power supply. Single-phase or 3-phase AC electric power with a frequency of 50 Hz or 60 Hz is fed into the power supply. Afterwards, the rectifier and the inverter realize the efficient conversion and control of electric energy from the fixed frequency AC to DC and then to a frequency-variable AC with the help of switching mode semiconductor power switches.

Rectifiers and inverters can both be classified into two groups: voltage-source type and current-source type. A further explanation of the resonant circuit focuses on a voltage-source rectifier and a voltage-source inverter. A voltage-source rectifier is applied to convert the AC voltage into DC voltage and a voltage-source inverter is connected after the rectifier in order to convert the DC voltage to a single-phase frequency-adjustable AC voltage. The controllable switches in the inverter switch on and off at the operating frequency f with a duty ratio of 50%, which results in a square voltage wave at the inverter output. The resonant circuit usually consists of inductors, capacitors and their parasitic resistors in series, parallel or series-parallel connections. A resonant frequency f_0 can be determined by the resonant circuit parameters and it can be adjusted by changing them. If the loaded quality factor is sufficiently high and the operating frequency f is close to the resonant frequency f_0, the impedance of the resonant circuit is low for the operating frequency component and quite high for the higher frequency components and, thus, the current flowing through the resonant circuit is approximately a sinusoidal wave equal to the frequency f, although the input voltage from the inverter is a square wave [8]. The sinusoidal AC flows through the induction coil, generates an electromagnetic field around the coil and heats the workpiece neighboring the coil. Finally, the control board receives the control commands, measures the sensed outputs from the induction heating system and generates the drive signals for the RF power supply. The DC output of the rectifier, the phase and frequency of the AC output and the heating temperature of the workpiece can be controlled. More explanation of the rectifier, the inverter and the resonant power converter can be found in [8,9]. In the next subsection, the experimental system for induction heating at the IVW will be explained in detail for a better understanding of the RF power supply and the resonant effect.

2.3 *IVW radio frequency power supply*

Figure 4 shows a schematic diagram, which can be used to depict the IVW RF power supply. In the supply, the three-phase 50 Hz AC voltages are connected through electromagnetic compatibility (EMC) filters to a six-pulse uncontrollable bridge rectifier that consists of six power diodes. A fixed DC voltage is obtained at the rectifier terminals. A filter choke is connected

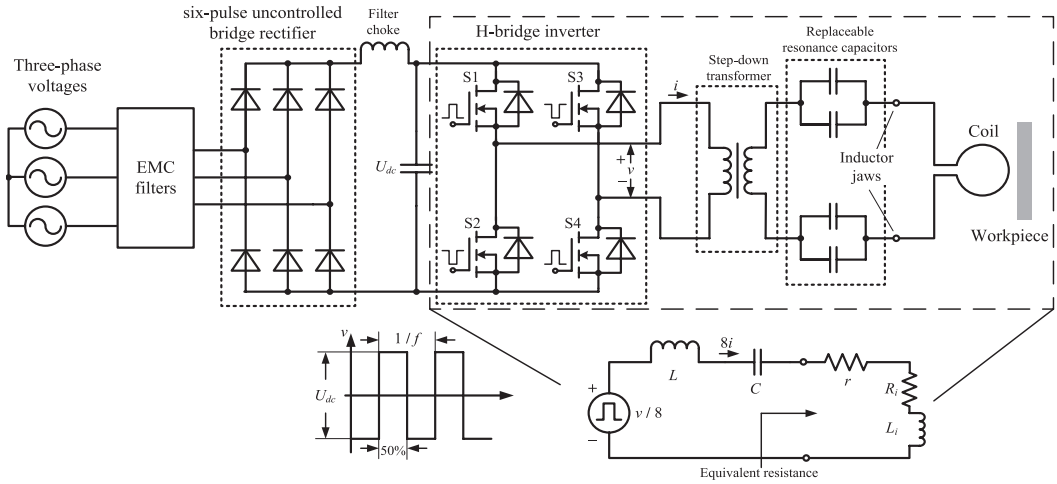

Figure 4: Schematic diagram of the RF power supply at the IVW.

to block high-frequency AC while allowing DC to pass and a capacitor is used to stabilize the DC-link voltage U_{dc}. The H-bridge inverter consists of four bi-directional switches S1, S2, S3 and S4. Each switch is composed of a high-speed power MOSFET and an anti-parallel diode. By assigning S1 and S4 with ON signals and S2 and S3 with OFF signals for half of the switching period 1/*f* and vice versa for another half period, a square symmetric voltage wave *v* with fixed amplitude is generated at the inverter output. A single-phase step-down transformer is used to reduce the output voltage. It induces a secondary voltage as a proportion of the primary voltage of the inverter with the ratio 1/8 and accordingly a secondary current as a proportion of the primary one with the ratio 8/1. To the secondary side of the transformation, four capacitors are distributed equally to the two inductor jaws of the power supply due to consideration of symmetry. Finally, the induction coil is connected to the inductor jaws to complete the circuit loop. For the whole system, water-cooling is used to remove the additional heat generated by the electrical components in the RF power supply as well as the coil.

An equivalent series-resonant circuit is developed by converting the circuit parameters from the primary side to the secondary side, which is also shown in the lower part of Figure 4. *v*/8 and 8*i* are the converted voltage from the inverter and the converted current in the resonant circuit. The inductor *L* is introduced by the transformer and *C* is the total capacitance of the four series-parallel capacitors. r is the sum of the on-resistance of the MOSFET and the parasitic resistance of the capacitor and the inductor. R_i is the load resistance from the coil and the workpiece and L_i is the load inductance. Some important parameters of the series-resonant circuit can be defined as follows: The resonant frequency

$$\omega_0 = \frac{1}{\sqrt{(L+L_i)C}}.$$

The unloaded quality factor

$$Q_0 = \frac{\omega_0 L}{r}.$$

The loaded quality factor

$$Q_L = \frac{\omega_0 (L+L_i)}{r+R_i} = \frac{1}{\omega_0 C(r+R_i)}.$$

The input impedance of the series-resonant circuit is

$$\begin{aligned}\mathbf{Z} &= (R_i + r) + j[\omega(L+L_i) - \frac{1}{\omega C}] \\ &= (R_i + r)[1 + jQ_L(\frac{\omega}{\omega_0} - \frac{\omega_0}{\omega})] \\ &= R + jX\end{aligned}$$

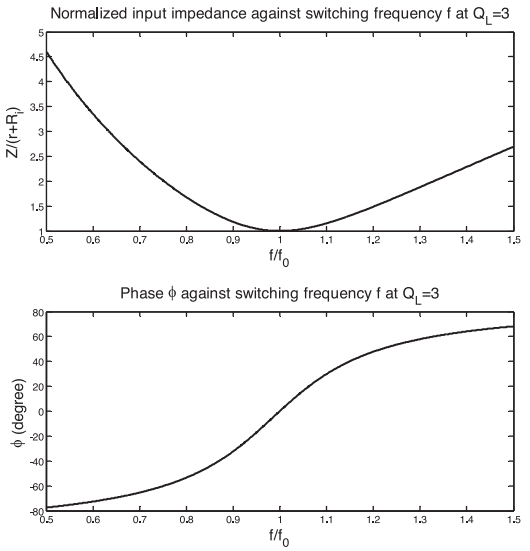

Figure 5: Input impedance of the series-resonant circuit against frequency f/f_0 at fixed loaded quality factor $Q_L = 3$.

where

$$Z = |\boldsymbol{Z}| = (r + R_i)\sqrt{1 + Q_L^2(\frac{\omega}{\omega_0} - \frac{\omega_0}{\omega})^2}$$

$$\phi = \arctan[\mathrm{Q_L}(\frac{\omega}{\omega_0} - \frac{\omega_0}{\omega})]$$

$$R = r + R_i = Z\cos\varphi$$

$$X = Z\sin\varphi\,.$$

$\omega = 2\pi f$ and describes the switching speed of the inverter MOSFETs. In the setup, the frequency of the coil current can be adjusted by changing the switching frequency f of the MOSFETs, replacing the applied transformer and the capacitors C. With respect to a realistic loaded quality factor (Q_L = 3) for the power supply, the corresponding characteristic plots for the input impedance can be derived, which are shown in Figure 5. When the square voltage with the switching frequency f approaches the resonance point f_0, the input impedance reaches its minimum value while the impedances to other voltage harmonics are larger. It explains why the current through the series-resonant circuit approximately appears as a sinusoidal wave and inevitably contains certain harmonics or distortion.

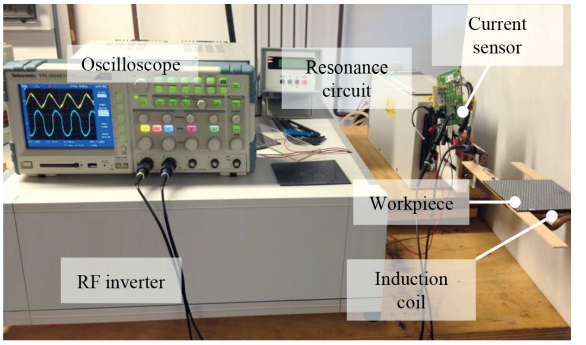

Figure 6: Overall experimental hardware setup.

3 Current Measurement Method

In this part, the measurement setup for the coil current and the voltage across the coil is presented.

3.1 *Sensor board selection*

The coil current is measured by a sensor board CMS3100 from Sensitec with a high bandwidth above 2 MHz. Other forms of current measurement equipment, such as current probes or current monitors, are 10 to 100 times more expensive and larger in size prohibiting permanent installment on the inverter itself. The CMS3100's measurement is based on the magneto-resistive effect and has the advantages of a bandwidth greater than 2 MHz, compact size and high accuracy. An oscilloscope with multiple channels and an internal rechargeable battery is used to simultaneously measure the voltage signal obtained from the sensor board and the coil voltage through the test probes. The voltage sources for the sensor and the oscilloscope have their own floating grounds, GND1 and GND2. To reduce the noise in the measured signals and, GND1 and GND2 are connected together.

3.2 *Sensor board installation*

A shown in Figure 6, the transformer and resonant capacitors are integrated into the resonance circuit in the power supply. A detailed connection setup for installing the current sensor board to the induction coil is presented in Figure 7 and Figure 8. The coil is extended by an additional copper-plastic structure composed of two copper terminals and one plastic insulation structure in order to redirect the coil current

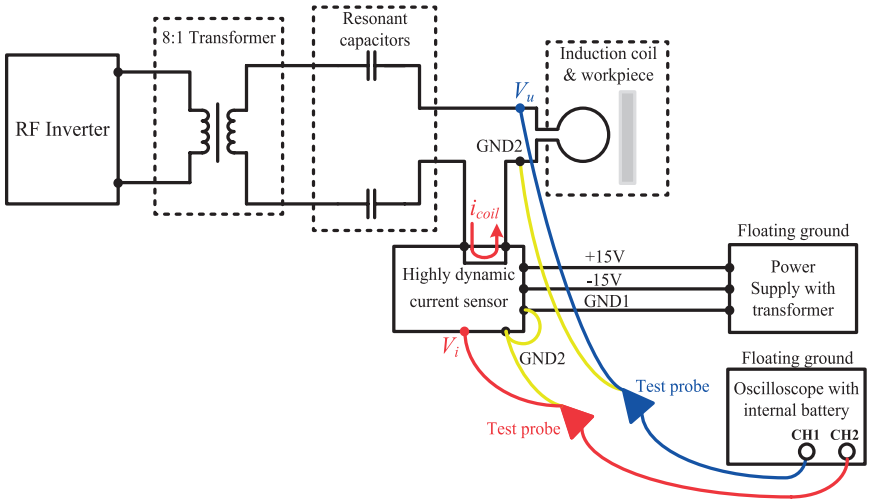

Figure 7: Schematic showing the connections between components of the experimental system.

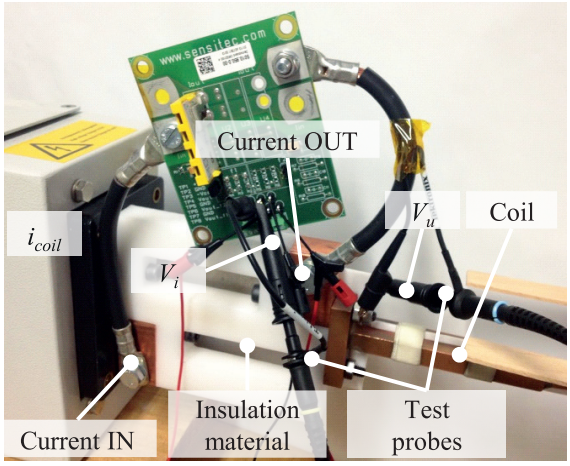

Figure 8: Series connection of the sensor board to the induction coil.

flow. The coil current can flow from the copper terminal 'Current IN', through the current sensor board and into the copper terminal 'Current OUT', as shown in Figure 8. The white block is an insulating plastic structure that is installed between the two copper terminals for additional support.

3.3 *Measurement output and results*

Four of the experimental results are selected and presented in this section. In these four experiments, a large spiral coil is used to heat a 100 x 100 mm pre-consolidated carbon fiber polyetheretherketone (CF/PEEK) laminate (TohoTenax TPCL PEEK-HTA40) with a thickness of 2.17 mm to a temperature well below its melt temperature of 343°C. The laminate is produced from 7 plies of a continuous carbon fiber 5H-satin weave reinforcement structure uniformly stacked and yields a composite fiber volume fraction of 50%. The amplitude and frequency of the coil current are controlled to different values and the distance between the coil and the CF/PEEK plate is adjusted to either 7 mm or 14 mm, as listed in Table 1.

Table 1: Experimental settings used for the four tests

	Coupling distance (mm)	Frequency (kHz)	Displayed current (A)	Measured current (A)
Test 1	7	458	24.8	23.35
Test 2	14	453	24.8	25.45
Test 3	7	372	40	38.21
Test 4	14	370	40	33.11

In Table 1, the measured current through the coil changes with respect to different heating frequencies and coupling distances, which actually reflects the fact that the heating effect differs among the four experimental settings. However, the displayed current values do not always change according to different settings. If the displayed values are used in the simulation model, the associated results can hardly be precise.

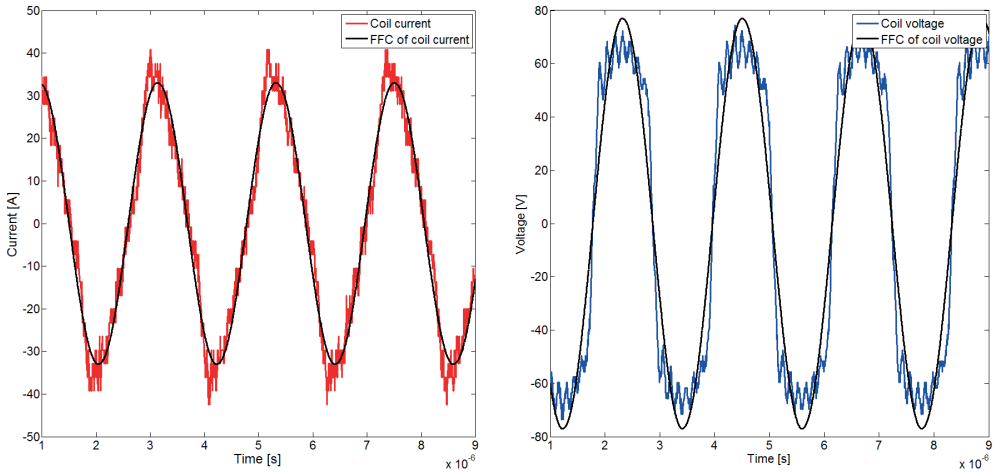

Figure 9: Test 1: spiral coil 23.35 A, 458 kHz, 7 mm coupling distance, CF/PEEK plate.

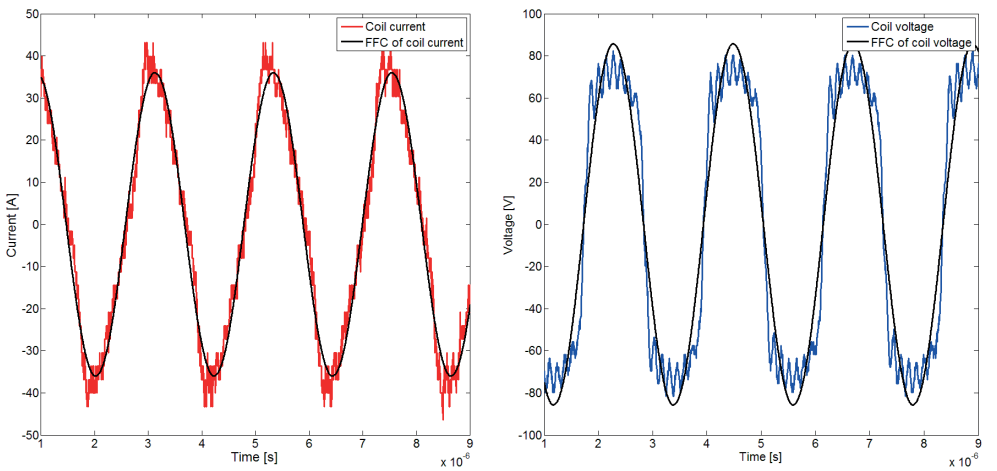

Figure 10: Test 2: spiral coil 25.45 A, 453 kHz, 14 mm coupling distance, CF/PEEK plate.

The waveforms of the coil current and voltage from the four tests are shown in Figure 9 to Figure 12. In the figures, the red curve shows the measured coil current and the blue one corresponds to the measured coil voltage. It can be seen that both coil voltage and current are not purely sinusoidal waveforms and that they contain their fundamental frequency components (FFCs) along with odd-order harmonics. The black curves in the figures therefore indicate the extracted FFCs derived from the Fourier transform. In fact, according to classical power theory, the power from the FFCs of the current and voltage is the most dominant contributor to the heating up of the workpiece. The total harmonic distortion (THD) is commonly used to characterize the power quality of the electric power and can be defined as the ratio of the sum of the powers from all the harmonic components to the power of the fundamental frequency. The corresponding THD values for all the current and voltage waveforms measured can be found in Table 2.

Table 2: Measured data from the four tests

		Test 1	**Test 2**	**Test 3**	**Test 4**
Coil current	Frequency (kHz)	458	453	372	370
	RMS value (A)	23.35	25.45	38.21	33.11
	THD (%)	15.94	15.66	13.99	13.18
Coil voltage	RMS value (V)	54.46	60.61	78.04	68.66
	THD (%)	25.53	26.60	23.71	24.07

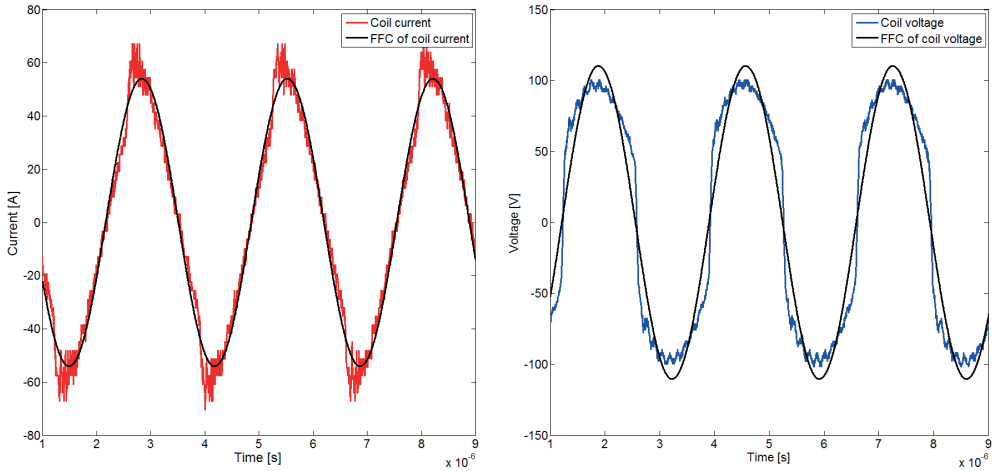

Figure 11: Test 3: spiral coil 38.21 A, 372 kHz, 7 mm coupling distance, CF/PEEK plate.

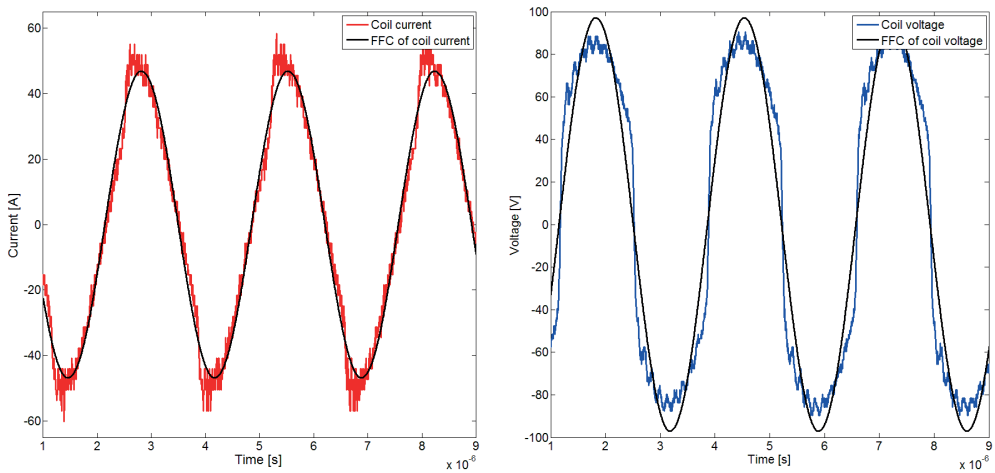

Figure 12: Test 4: spiral coil 33.11 A, 370 kHz, 14 mm coupling distance, CF/PEEK plate.

4 Modelling and Analysis Tools

In this work two types of modelling tools have been used. The first is based on principles used in electrical circuit analysis and considers the estimation of the load impedance by analyzing the measured coil current and voltage waveforms as described in section 3. The second is based on geometric modelling techniques using multiphysics finite element software codes. Both types of modelling approaches can help to understand more deeply the nature of the induction heating system and can even be used for prediction and parameter variation studies.

4.1 *Load impedance circuit analysis modelling*

The induction heating process can be modelled by the transformer principal. As already mentioned in section 2.3, the induction coil is similar to the primary side of a transformer and the workpiece can be seen as equivalent to the secondary side of the transformer. The heated workpiece can be converted to the transformer primary side so that it can be represented as an impedance combined with the induction coil. Note that the "transformer" described here is not a real transformer as the 8:1 step-down one present in the power supply. The value of the equivalent impedance

shows a nonlinear behavior that can be influenced by the amplitude and frequency of the induced current and the temperature. The load impedance can be assumed as an electrical model with a series connected resistance and inductance. The equivalent resistance and inductance can be estimated by analyzing the measured coil current and voltage. The waveforms of the coil current and voltage can be recorded by the oscilloscope and the fundamental frequency components (FFC) of the current and voltage are extracted by Fourier transform. Therefore, the amplitudes of the FFC current and voltage as discussed in section 3 and their phase difference can be obtained. The corresponding resistance and inductance can then be calculated.

The calculated equivalent resistance and inductance under various induction heating conditions can directly reflect the electrical properties in this studied process. Therefore, an analytical model of the induction heating with respect to the shape of the induction coil, the workpiece material, the induction distance, the current frequency and the workpiece temperature can be developed to quantify the complicated induction heating process following a sufficient number of measurements. With the help of this induction heating model, a closed-loop controller can be designed and implemented to achieve a more precise heating effect.

Two additional important variables, the real power and the reactive power, can also be derived from the model and can indicate the amount of energy delivered to the workpiece per second. The real power comes from the equivalent resistance part that is consumed in the form of heat while the reactive power is introduced by the inductance part that oscillates between the inductor and the power supply. The active power actually heats the workpiece while the reactive power generates a magnetic field to support transfer of the real power from the induction coil to the workpiece. The values of the required real power and the corresponding reactive power reveal the real amount of the power required for heating the workpiece and provide a guideline on parameter design of the RF inverter. A more detailed look into this is left as the basis for future work.

4.2 *3D finite element multiphysics modelling*

Modelling on the basis of full three dimensional geometry and material properties obtained by specific material characterization tests (mechanical, thermal and electromagnetic) can also provide a powerful tool for understanding and prediction. Many finite element software codes have today become capable of multiphysics simulations where the interaction between mechanical, thermal and electromagnetic effects can be considered. Duhovic et al. [10-13] have already investigated several such cases using LSTC's LS-DYNA and COMSOL AB's COMSOL multiphysics, where the aim has been to simulate the resulting Joule heating effect in thermoplastic composite plates and induction welding setups.

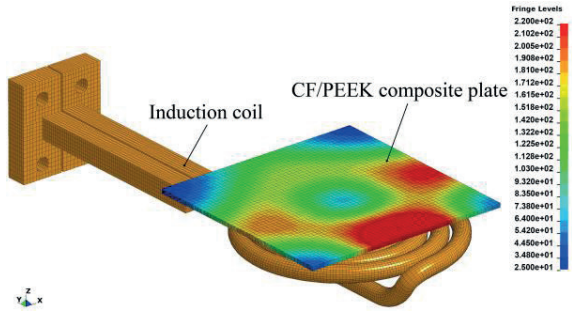

Figure 13: LS-DYNA FEA simulation of Joule heating in a CF/PEEK plate coil current 23.35 A, frequency 458 kHz and 7 mm coupling distance.

Using the input data gathered from the current measurements performed together with a wide range of material properties, more accurate full 3D models can be built up and used to predict the joule heating effect which occurs during induction heating. In this work, the complex case of a CF/PEEK plate together with a large spiral coil has been chosen and modelled in LS-DYNA as shown in Figure 13 for one of the four test cases considered. In such models, composite material inhomogeneity is currently not considered as the repeating unit cell structure of the composite's weave reinforcement structure is usually small enough to produce a homogenized heating effect at the macro-scale (laminate level). This can be seen in Figure 14, where no apparent pattern resulting from the reinforcement weave structure can be observed. For materials with larger yarns and yarn spacing (e.g. 5 mm or greater) or when the coil size to yarn size and spacing ratio is very small, then the finite element mesh can be separated into discrete fiber and matrix material element volumes to better represent the heat distribution.

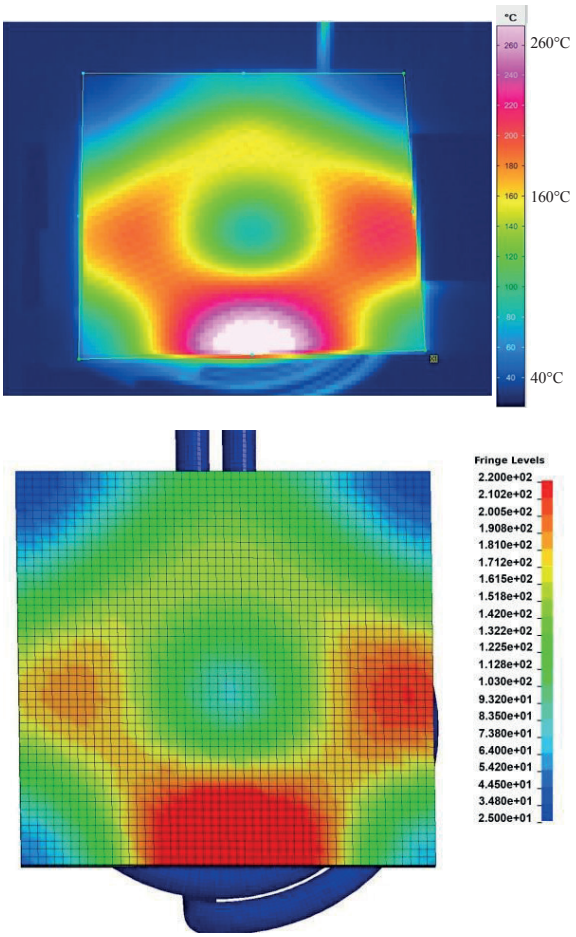

Figure 14: Comparison between thermal camera and simulated Joule heating temperature contours of a CF/PEEK plate coil current 23.35 A, frequency 458 kHz and 7 mm coupling distance.

The size of the coil has been deliberately chosen to be slightly larger than the plate to ensure that the electromagnetic "edge effects" which occur in reality and result in a more complex heating pattern, can also be reproduced in the simulation. To verify the simulation models, the experimental and simulated Joule heating results can be compared by considering entire surface infrared thermography images, see again Figure 14, as well as the maximum and average temperature development on the surface of the composite plate opposite to the side exposed to the coil, Figure 15. Note that the temperature unit system used in all cases is degrees Celsius.

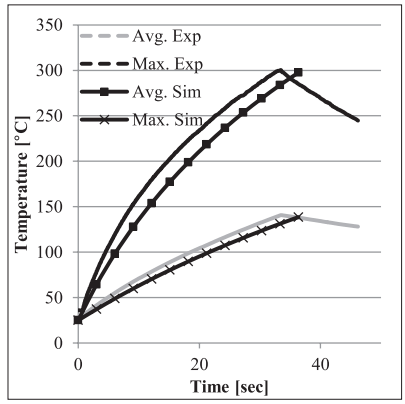

Figure 15: Comparison between simulated and measured average and maximum temperatures for coil current 23.35 A, frequency 458 kHz and 7 mm coupling distance.

It can be seen that a very good agreement of the heating pattern as well as the maximum and minimum temperatures and their locations can be achieved. In addition to Joule heating simulations, the nature of the current and voltage waveforms can also be investigated in detail using the eddy current solver available in LS-DYNA. In these types of simulations, the current or voltage waveforms measured and calculated, as shown in section 3, are used as part of the simulation input which considers several cycles of the oscillating system over a time period in the order of microseconds (several time periods of the waveform). If the current waveform is used as input, then the simulation outputs the corresponding voltage waveform and vice versa. This allows the calculation of the active and reactive power components discussed in section 4.1, to be predicted by the FEA simulation and can then be directly compared with the modelling approach used in 4.1. This again provides further basis for future work.

5 Conclusions

The frame work for a more thorough investigation of the induction welding of thermoplastic composites has been discussed here. First, the state of the art of induction welding and its systems has been presented focusing on the most important component, the RF power supply. Second, current waveform measurement using a magnetoresistive measurement board has been described in terms of implementation onto existing

induction power supply equipment. The procedure for obtaining the FFC from the measurement data by FFT has been shown. Using the accurately measured current data, modelling analysis tools including load impedance circuit modelling and 3D geometric finite element modelling have both been proposed. In the case of FEA modelling excellent prediction of the heating behavior in CF/PEEK laminates has been shown, even in the case of a more complex case heating scenario where edge effect heating is present.

Acknowledgments

The authors would like to thank Dr. Günter Uhl for his help during this work and Sensitec GmbH for the donation of the current measuring board.

References

[1] P. Mitschang, R. Rudolf, and M. Neitzel, "Continuous Induction Welding Process, Modelling and Realisation," *Journal of Thermoplastic Composite Materials*, vol. 2, pp. 127-153, 2002.

[2] A. K. Miller, C. Chang, A. G. M. Payne, E. Menzel, and A. Peled, "The nature of induction heating in graphite-fiber, polymer-matrix composite materials," *Sampe Journal*, vol. 4, pp. 37-54, 1990.

[3] R. Rudolf, P. Mitschang, and M. Neitzel, "Induction heating of continuous carbon-fibre-reinforced thermoplastics," *Composites Part A: Applied Science and Manufacturing*, vol. 11, pp. 1191-1202, 2000.

[4] S. Zinn and S. L. Semiatin, "Coil design and fabrication: basic design and modifications," *Heat Treating*, 1988.

[5] D. Puyal, C. Bemal, J.-M. Burdio, I. Millan, and J. Acero, "Dual 1.5-MHz 3.5-kW versatile half-bridge series-resonant inverter module for inductive load characterization," in *Applied Power Electronics Conference, APEC 2007 - Twenty Second Annual IEEE*, 2007, pp. 1133-1139.

[6] D. Puyal, C. Bernal, J.-M. Burdio, J. Acero, and I. Millan, "Methods and procedures for accurate induction heating load measurement and characterization," in *Industrial Electronics, 2007. ISIE 2007. IEEE International Symposium on*, 2007, pp. 805-810.

[7] V. Rudnev, D. Loveless, R. L. Cook, and M. Black, *Handbook of Induction Heating*, 2002.

[8] M. Kazimierczuk, *Resonant power converters*, 2011.

[9] B. K. Bose, *Modern power electronics and AC drivers*, 2002.

[10] I. Caldichoury, P. L'Eplattenier, and M. Duhovic, "LS-DYNA R7: coupled multiphysics analysis involving electromagnetism (EM), incompressible CFD (ICFD) and solid mechanics thermal solver for conjugate heat transfer problem solving," in *Proceedings of the 9th European LS-DYNA users conference*, 2013.

[11] M. Duhovic, I. Caldichoury, P. L'Eplattenier, P. Mitschang, and M. Maier, "Advances in simulating the joining of composite materials by electromagnetic induction," in *Proceedings of the 9th European LS-DYNA users conference*, 2013.

[12] M. Duhovic, M. Hümbert, P. Mitschang, M. Maier, I. Caldichoury, and P. L'Eplattenier, "Further advances in simulating the processing of composite materials by electromagnetic induction," in *Proceedings of the 13th international LS-DYNA users conference*, 2014.

[13] M. Duhovic, L. Moser, P. Mitschang, M. Maier, I. Caldichoury, and P. L'Eplattenier, "Simulating the joining of composite materials by electromagnetic induction," in *Proceedings of the 12th international LS-DYNA users conference*, 2012.